Electronic supplementary materials *Mendeleev Commun.*, 2022, **32**, 68-70

Reactions of an aluminium(I) diketiminate compound with arenas

Anton Dmitrienko, Melanie Pilkington and Georgii I. Nikonov

Contents

1. General considerations

All manipulations were carried out under the inert atmosphere of dry nitrogen using conventional Schlenk technique or in an MBraun glovebox containing an atmosphere of purified nitrogen, unless stated otherwise. All solvents used for the synthesis were dried and purified with the employment of a Grubbs-type Pure-Solv^{TM} solvent purification system. Benzene-d_6 was dried over K/Na alloy and then distilled into a sealed glass vessel that was kept in the glovebox. Reagents for the reactions were purchased from commercial supplies and processed as received, unless stated otherwise. Potassium graphite was prepared by weighing corresponding amount of graphite with the following drying of the substrate over two hours in a Schlenk-type tube. Potassium chunks were stripped of kerosene with hexane with the following transfer in a Schlenk tube upon evacuation of the residual solvents and gasses in vacuo. Finely cut pieces of potassium metal were carefully dropped into the ampule equipped with a large stirring bar and pre-dried graphite. The reaction vessel was submerged into the oil bath heated up to 120 °C with a stirring plate. Once potassium melted, the reaction vessel was connected to the Schlenk dual manifold and the manual stirring with a long spatula was carried out under steady flow of dry nitrogen. **Caution!** The resulting fine powder of potassium graphite is highly pyrophoric, so that the optimal flow of nitrogen should be supplied all the time the reaction vessel is opened to the atmosphere of air. Compound **5** was synthesized in compliance with the established procedure.[†] The resulting crude material was centrifuged from the mother liquor in toluene and then washed with hexanes and centrifuged one more time with Beckman Coulter Allegra X-30R centrifuge at -20°C (10000 RPM, 1 hour, sealed vessel). NMR spectra were recorded on a Bruker Avance III HD 600 MHz spectrometer at the room temperature unless stated otherwise. Processing and interpretation of spectroscopic data were performed with MestReNova software (v.10.0.2-15465). Spectroscopic data was referenced to residual solvent signals as internal standards. Assignment of ^{13}C resonances was based on interpretation of ^{1}H-^{13}C-HSQC and ^{1}H-^{13}C-HMBC spectra. Elemental analyses were conducted by the analytical laboratory for Environmental Science Research and Training (ANALEST). Samples were calibrated against thermal standard acetanilide: C (71.09%), H (6.71%), N (10.36%) before, during and after analysis. The analyses were run on ThermoFisher Flash 2000 analyzer with Mettler MT5 balance.

List of abbreviations: NMR – nuclear magnetic resonance, HSQC – heteronuclear single quantum coherence, HMBC – heteronuclear multiple bond correlation, s – singlet, d – doublet, dd – doublet of doublets, ddd –

[†] C. Cui, H. W. Roesky, H.-G Schmidt, M. Noltemeyer, H. Hao, F. Cimpoesu. *Angew. Chem. Int. Ed.* 2000, **39**, 4274.

doublet of doublets of doublets, t – triplet, td – triplet of doublets, dt – doublet of triplets, hept – heptet, m – multiplet, ppm – part per million, SC-XRD – single crystal x-ray diffraction, MW – molecular weight.

2. Procedure for synthesis of 7

Naphthalene (0.0320 g, 0.25 mmol) was dissolved in toluene (1 ml) and then added to the concentrated solution of **5** (0.1111 g, 0.25 mmol) in toluene (1 ml) under constant stirring. The reaction mixture was heated at 40 °C for 8 hours. The color of the solution developed a yellow hue overnight, while significant amount of precipitate crushed out of solution. Product **7** was recrystallized from diethyl ether solution at -30°C to give pure **7** (MW = 572.82 g mol^{-1}). Yield: 0.0906g (63%).

^{1}H NMR (600 MHz, C_6D_6) δ 7.15 – 7.12 (m, 1H, C_6H_3), 7.10 (m, 2H, C_6H_3), 6.95 (m, 1H, C_6H_3), 6.92 (dd, $^{3}J_{H\text{-}H}$ = 5.4, $^{4}J_{H\text{-}H}$ = 3.2 Hz, 2H, C_6H_4, arom.), 6.88 (d,$^{3}J_{H\text{-}H}$ = 7.6 Hz, 2H, C_6H_3), 6.74 (dd, $^{3}J_{H\text{-}H}$ = 5.4, $^{4}J_{H\text{-}H}$ = 3.2 Hz, 2H, C_6H_4, arom.), 5.73 (dd, $^{3}J_{H\text{-}H}$ = 4.7, $^{4}J_{H\text{-}H}$ = 3.5 Hz, 2H, C_6H_4), 4.82 (s, 1H, C*H*), 3.72 (dd, $^{3}J_{H\text{-}H}$ = 4.7, $^{4}J_{H\text{-}H}$ = 3.5 Hz, 2H, C_6H_4), 3.21 (hept, $^{3}J_{H\text{-}H}$ = 6.7 Hz, 2H, C*H*$(CH_3)_2$), 3.15 (hept, $^{3}J_{H\text{-}H}$ = 6.7 Hz, 2H, C*H*$(CH_3)_2$), 1.51 (d+s, 6H+3H, $^{3}J_{H\text{-}H}$ = 6.7 Hz, CH(C*H*$_3)_2$ + C*H*$_3$), 1.44 (d, $^{3}J_{H\text{-}H}$ = 6.7 Hz, 6H, CH(C*H*$_3)_2$), 1.38 (s, 3H, C*H*$_3$), 1.05 (d, $^{3}J_{H\text{-}H}$ = 6.7 Hz, 6H, CH(C*H*$_3)_2$), 0.96 (d, $^{3}J_{H\text{-}H}$ = 6.7 Hz, 6H, CH(C*H*$_3)_2$).

^{13}C NMR (151 MHz, C_6D_6) δ 171.5 (*C*CH_3, q.), 170.9 (*C*CH_3, q.), 144.6 (*C*$_6H_4$, q.), 142.6 (*C*$_6H_3$, q.), 142.5 (*C*$_6H_3$, q.), 140.6 (*C*$_6H_3$, q.), 137.9 (toluene), 129.3 (toluene), 128.6 (*C*$_6H_3$), 127.6 (*C*$_6H_3$), 127.3 (*C*$_6H_3$), 125.7 (toluene), 125.6 (*C*$_6H_4$), 124.7 (*C*$_6H_3$), 124.3 (*C*$_6H_3$), 122.0 (*C*$_6H_4$), 121.2 (*C*$_6H_4$), 97.5 (*C*H), 44.4 (*C*$_6H_4$), 28.9 (*C*H$(CH_3)_2$), 28.7 (*C*H$(CH_3)_2$), 25.1 (CH(*C*$H_3)_2$), 25.0 (CH(*C*$H_3)_2$), 24.1 (CH(*C*$H_3)_2$), 23.7 (CH(*C*$H_3)_2$), 21.4 (toluene).

Elemental analysis (%): Calculated: C (81.78), H (8.62), N (4.89). Experimental: C (82.15), H (8.58), N (4.12).

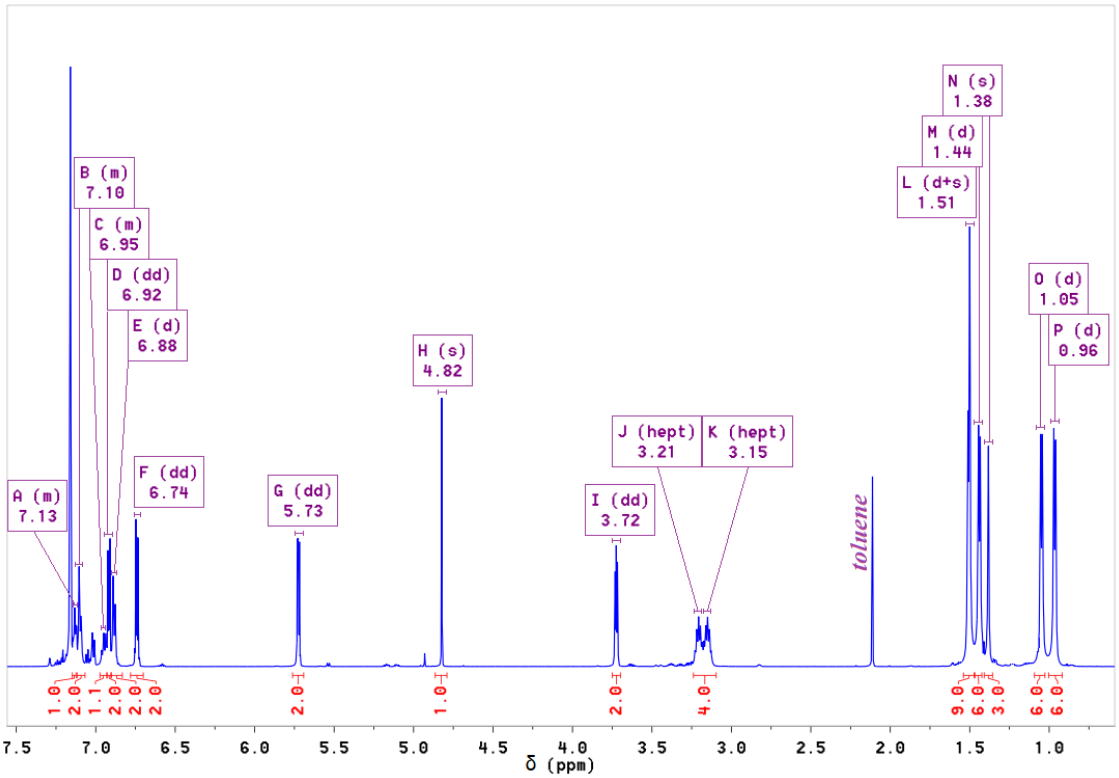

Figure S1. ^{1}H NMR spectrum of compound **7** in C_6D_6.

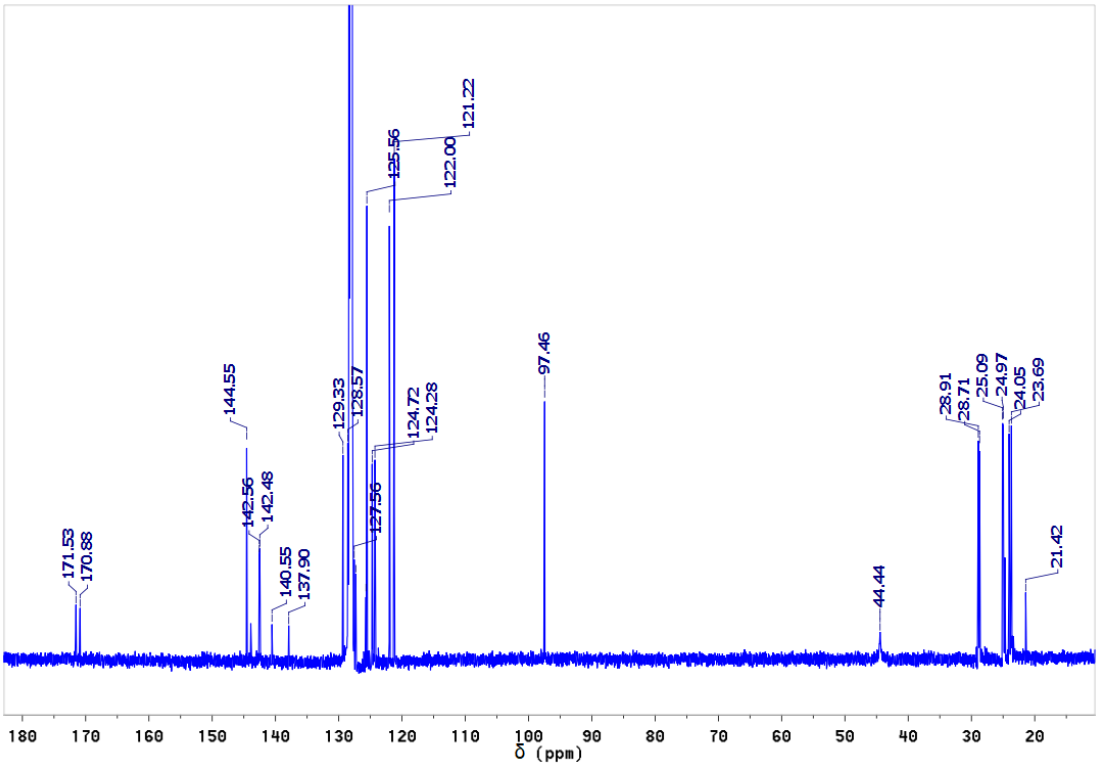

Figure S2. ^{13}C NMR spectrum of compound **7** in C_6D_6.

3. Procedure for synthesis of 8c

Anthracene (0.0393 g, 0.22 mmol) was added as a slurry in wet diethyl ether (1 ml) to the concentrated solution of compound **5** (0.0981 g, 0.22 mmol) in Et_2O (3 ml) under constant stirring. The colour of reaction mixture developed a yellow hue overnight, while significant amount of solid precipitated from the solution. **8c** was recrystallized from diethyl ether solution at -30°C to give pure **8c** (MW = 640.89 g mol^{-1}). Yield: 0.0296 g (21%).

^{1}H NMR (600 MHz, C_6D_6) δ 7.19 (t, $^3J_{H-H}$ = 7.6 Hz, 2H, C_6H_3), 7.14 (m, 2H, C_6H_3), 7.03 (d, $^3J_{H-H}$ = 7.4 Hz, 2H, C_6H_4), 6.93 (dd, $^3J_{H-H}$ = 7.6, $^4J_{H-H}$ = 1.5 Hz, 2H, C_6H_3), 6.84 (td, $^3J_{H-H}$ = 7.4, $^4J_{H-H}$ = 1.1 Hz, 2H, C_6H_4), 6.53 (t, $^3J_{H-H}$ = 7.5 Hz, 2H, C_6H_4), 6.11 (d, $^3J_{H-H}$ = 7.5 Hz, 2H, C_6H_4), 4.91 (s, 1H, C*H*), 4.36 (d, $^2J_{H-H}$ = 15.8 Hz, 1H, C(CH_2)C), 3.59 (d, $^2J_{H-H}$ = 15.8 Hz, 1H, C(CH_2)C), 3.48 (s, 1H, C(C*H*)C), 3.40 (hept, $^3J_{H-H}$ = 6.8 Hz, 2H, C*H*(CH_3)$_2$), 3.29 (hept, $^3J_{H-H}$ = 6.8 Hz, 2H, C*H*(CH_3)$_2$), 1.481 (d, $^3J_{H-H}$ = 7.1 Hz, 6H), 1.480 (s, 6H, CCH_3), 1.10 (d, $^3J_{H-H}$ = 6.8 Hz, 6H, CH(CH_3)$_2$), 1.09 (d, $^3J_{H-H}$ = 6.8 Hz, 6H, CH(CH_3)$_2$), 0.67 (d, $^3J_{H-H}$= 6.8 Hz, 6H, CH(CH_3)$_2$), 0.47 (s, 1H, OH).

^{13}C NMR (151 MHz, C_6D_6) δ 170.3 (CH_3*C*, q.), 145.1 (*C*$_6H_3$, q.), 143.4 (*C*$_6H_4$, q.), 142.6 (*C*$_6H_3$, q.), 142.2 (*C*$_6H_3$, q.), 135.0 (*C*$_6H_4$, q.), 127.5 (*C*$_6H_4$), 127.1 (*C*$_6H_4$), 125.6 (*C*$_6H_3$), 125.4 (*C*$_6H_4$), 125.1 (*C*$_6H_4$), 124.1 (*C*$_6H_3$), 122.6 (C_6H_3), 98.6 (*C*H), 40.9 (only in HSQC, C(*C*H)C), 38.5 C(*C*H_2)C, 29.3 (*C*H(CH_3)$_2$), 27.8 (*C*H(CH_3)$_2$), 25.1 (CH(*C*H_3)$_2$), 24.7 (CH(*C*H_3)$_2$), 24.3 (CH(*C*H_3)$_2$), 23.8 (CH(*C*H_3)$_2$), 23.6 (*C*CH_3).

Elemental analysis (%): Calculated: C (80.59), H (8.34), N (4.37). Experimental: C (80.14), H (8.30), N (3.86).

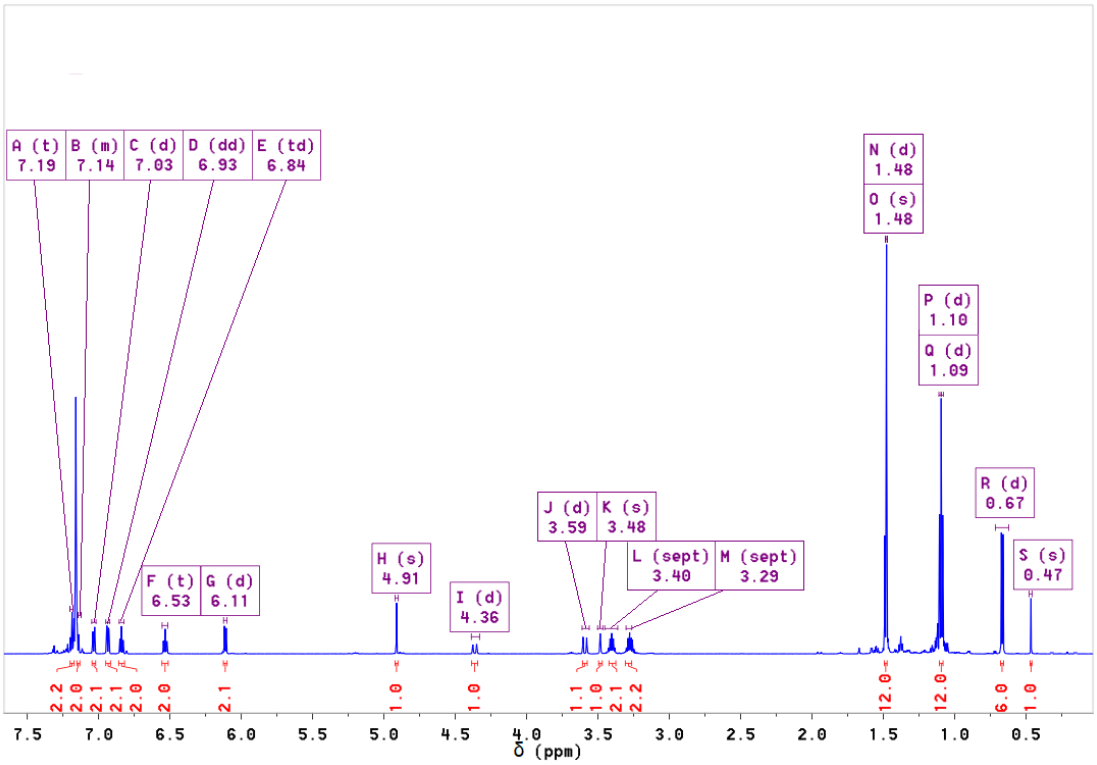

Figure S3. ^{1}H NMR spectrum of compound **8c** in C_6D_6.

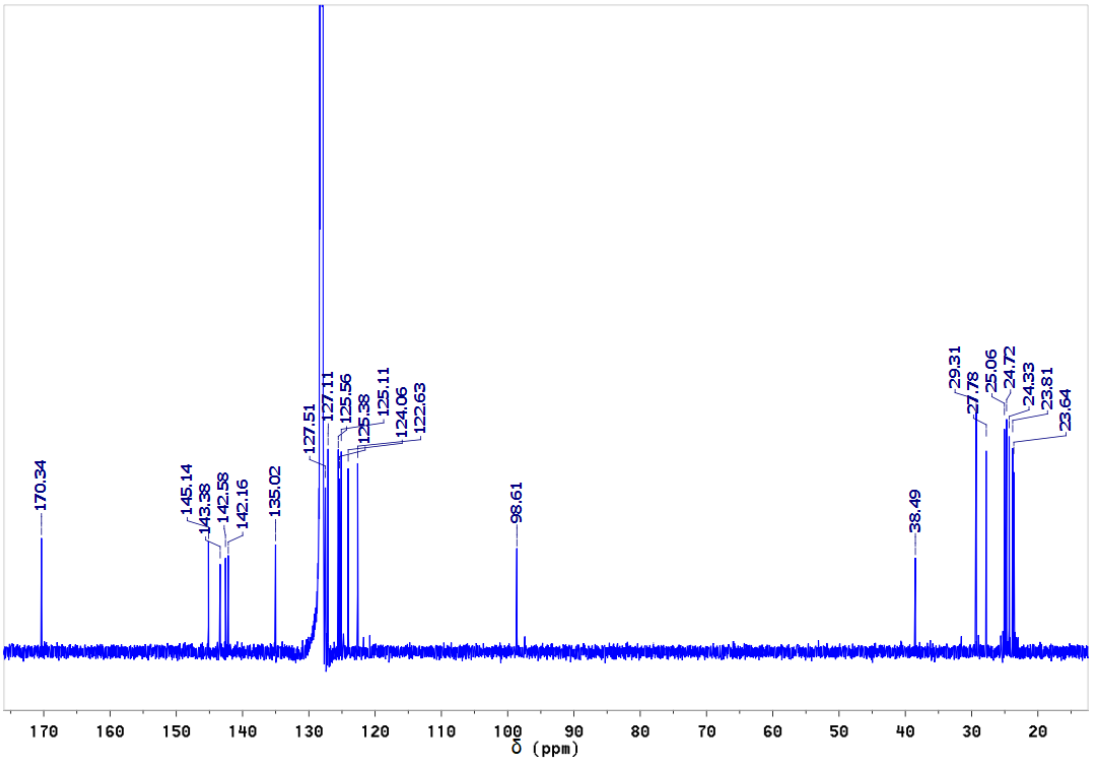

Figure S4. ^{13}C NMR spectrum of compound **8c** in C_6D_6.

4. Dynamic equilibrium between 5 and phenanthrene adduct 9

^{1}H NMR (600 MHz, C_6D_6) δ 8.25 (d, $^3J_{H\text{-}H}$ = 8.3 Hz, 1H, C_6H_4), 7.71 (d, $^3J_{H\text{-}H}$ = 8.3 Hz, 1H, C_6H_4), 7.34 (ddd, $^3J_{H\text{-}H}$ = 8.2, $^4J_{H\text{-}H}$ = 6.7, $^5J_{H\text{-}H}$ = 1.3 Hz, 1H, C_6H_4), 7.24 (ddd, $^3J_{H\text{-}H}$ = 8.2, $^4J_{H\text{-}H}$ = 6.7, $^5J_{H\text{-}H}$ = 1.3 Hz, 1H, C_6H_4), 7.14 (d, $^3J_{H\text{-}H}$ = 8.0 Hz, 1H, C_6H_2), 7.01 (d, $^3J_{H\text{-}H}$ = 8.0 Hz, 1H, C_6H_2), 6.86 (d, $^3J_{H\text{-}H}$ = 7.5 Hz, 1H, C_6H_3)*, 6.75 (t, $^3J_{H\text{-}H}$ = 7.5 Hz, 1H, C_6H_3)*, 6.45 (d, $^3J_{H\text{-}H}$ = 7.5 Hz, 1H, C_6H_3)*, 5.82 (td, $^3J_{H\text{-}H}$ = 6.3, $^4J_{H\text{-}H}$ = 1.7 Hz, 1H, C_6H_4 (dearom.)), 5.75 (td, $^3J_{H\text{-}H}$ = 6.3, $^4J_{H\text{-}H}$ = 1.7 Hz, 1H, C_6H_4 (dearom.)), 4.82 (s, 1H, C*H*), 4.50 (dd, $^3J_{H\text{-}H}$ = 6.3, $^4J_{H\text{-}H}$ = 1.4 Hz, 1H, C_6H_4 (dearom.)), 3.81 (dd, $^3J_{H\text{-}H}$ = 6.2, $^4J_{H\text{-}H}$ = 1.9 Hz, 1H, C_6H_4 (dearom.)), 3.24 (m. hept, $^3J_{H\text{-}H}$ = 6.8 Hz, 3H, C*H*$(CH_3)_2$), 2.74 (hept, $^3J_{H\text{-}H}$ = 6.8 Hz, 1H, C*H*$(CH_3)_2$), 1.57 (d, $^3J_{H\text{-}H}$ = 6.8 Hz, 3H, CH$(CH_3)_2$), 1.52 (d+s, $^3J_{H\text{-}H}$ = 6.8 Hz, 3H+3H, CH$(CH_3)_2$+CC*H*$_3$), 1.48 (d, $^3J_{H\text{-}H}$ = 6.8 Hz, 3H, CH$(CH_3)_2$), 1.33 (s, 3H, CC*H*$_3$), 1.08 (d+d, $^3J_{H\text{-}H}$ = 6.8 Hz, 6H, CH$(CH_3)_2$), 0.98 (d, $^3J_{H\text{-}H}$ = 6.8 Hz, 3H, CH$(CH_3)_2$), 0.80 (d, $^3J_{H\text{-}H}$ = 6.8 Hz, 3H, CH$(CH_3)_2$), 0.68 (d, $^3J_{H\text{-}H}$ = 6.8 Hz, 3H, CH$(CH_3)_2$).

*****Only three protons were found for C_6H_3 group. Other three signals are overlapped with C_6D_6 residual peak.

^{13}C NMR (151 MHz, C_6D_6) δ 171.4 (*C*CH_3, q.), 171.2 (*C*CH3, q.), 165.3 (NacNacAl), 143.8 (NacNacAl)**,** 142.8 (*C*$_6H_3$, q.), 142.4 (*C*$_6H_3$, q.), 142.3 (NacNacAl), 142.0 (*C*$_6H_3$, q.), 141.9 (*C*$_6H_2$, q.), 140.9 (*C*$_6H_3$, q.), 137.7 (*C*$_6H_2$, q.), 132.6 (phenanthrene), 131.7 (*C*$_6H_2$, q.), 130.9 (phenanthrene), 128.9 (phenanthrene), 128.8 (*C*$_6H_2$, q.), 128.5 (*C*$_6H_4$), 127.4 (NacNacAl), 127.3 (phenanthrene), 126.91 (*C*$_6H_3$), 126.87 (C_6H_3), 126.80 (*C*$_6H_4$, dearom.), 126.79 (phenanthrene), 125.1 (*C*$_6H_4$, dearom.), 124.9 (C_6H_3), 124.6 (*C*$_6H_3$), 124.4 (*C*$_6H_4$), 124.3 (NacNacAl + overlapped *C*$_6H_3$), 124.1 (*C*$_6H_3$), 123.9 (*C*$_6H_4$), 123.1 (phenanthrene), 122.6 (*C*$_6H_2$), 122.2 (*C*$_6H_4$), 122.1 (*C*$_6H_2$), 100.9 (NacNacAl), 97.7 (*C*H), 45.5 (C_6H_4, dearom.), 40.1 (*C*$_6H_4$, dearom.), 29.1 (NacNacAl), 29.0 (*C*H$(CH_3)_2$), 28.92 (*C*H$(CH_3)_2$), 28.89 (*C*H$(CH_3)_2$), 28.6 (*C*H$(CH_3)_2$), 25.2 (CH(*C*H$_3)_2$), 25.14 (NacNacAl), 25.05 (CH(*C*H$_3)_2$), 25.0 (CH(*C*H$_3)_2$), 24.63 (CH(*C*H$_3)_2$), 24.60 (CH(*C*H$_3)_2$), 24.5 (CH(*C*H$_3)_2$), 24.1 (C*C*H$_3$), 23.9 (NacNacAl), 23.9 (CH(*C*H$_3)_2$, 23.8 (NacNacAl), 23.6 (C*C*H$_3$), 23.4 (CH(*C*H$_3)_2$).

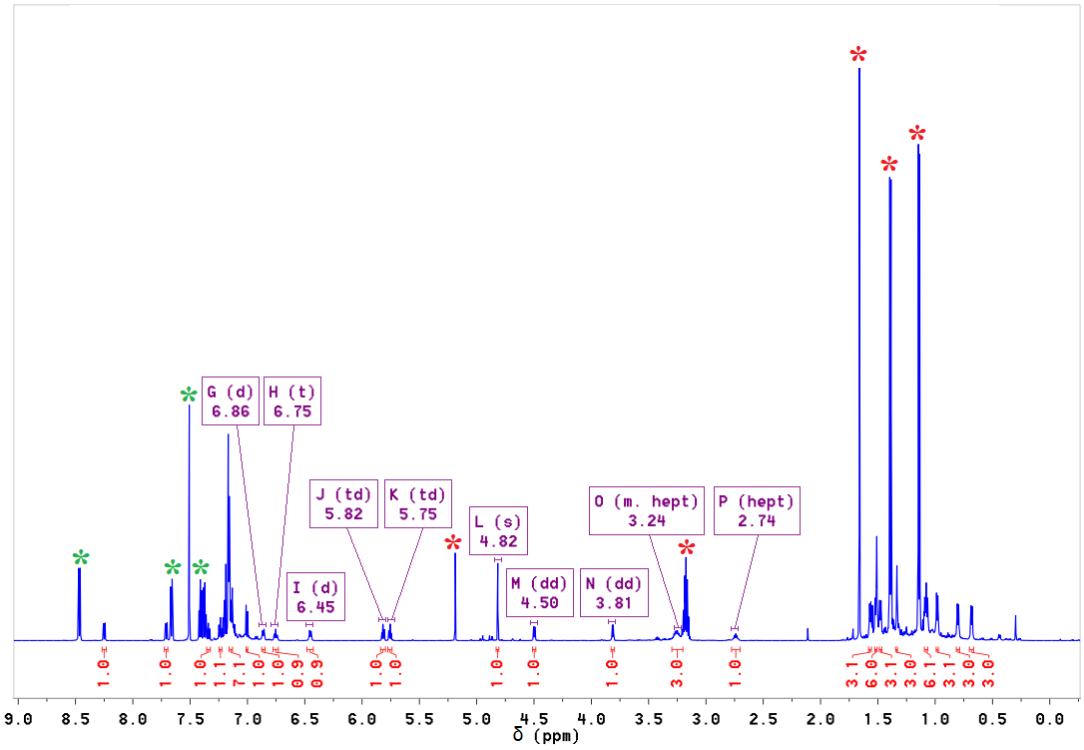

Figure S5. ^{1}H NMR spectrum of the equilibrium with phenanthrene in C_6D_6.

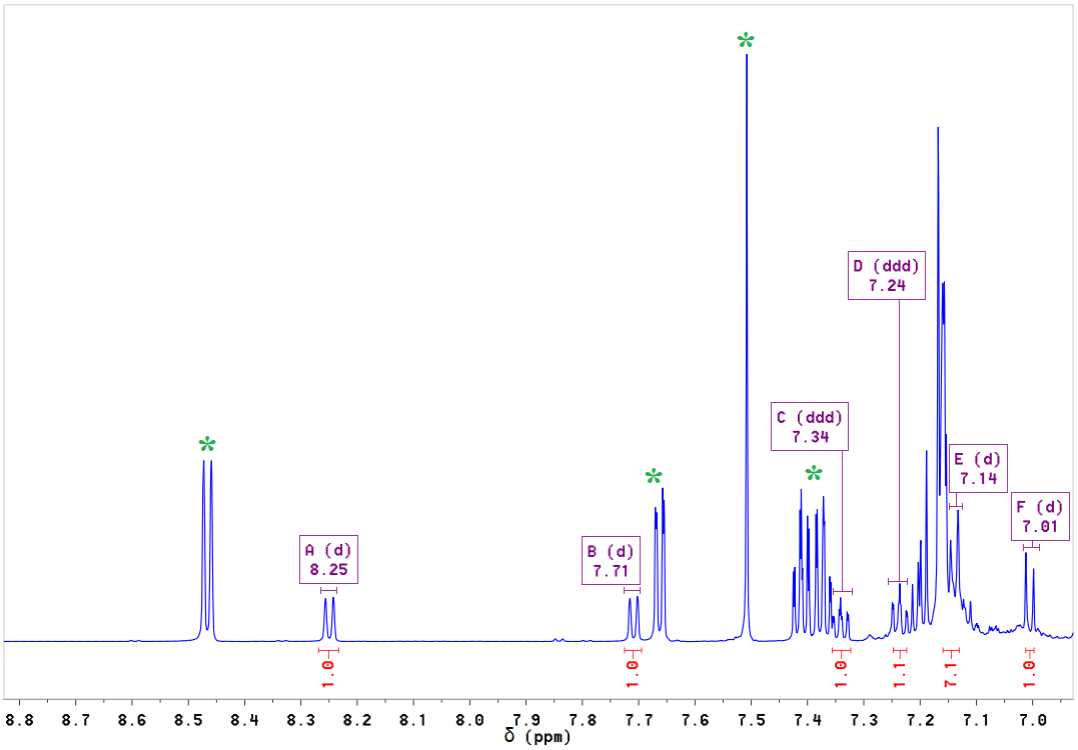

Figure S6. Selected weak field region of the ^{1}H NMR spectrum of the equilibrium with phenanthrene in C_6D_6.

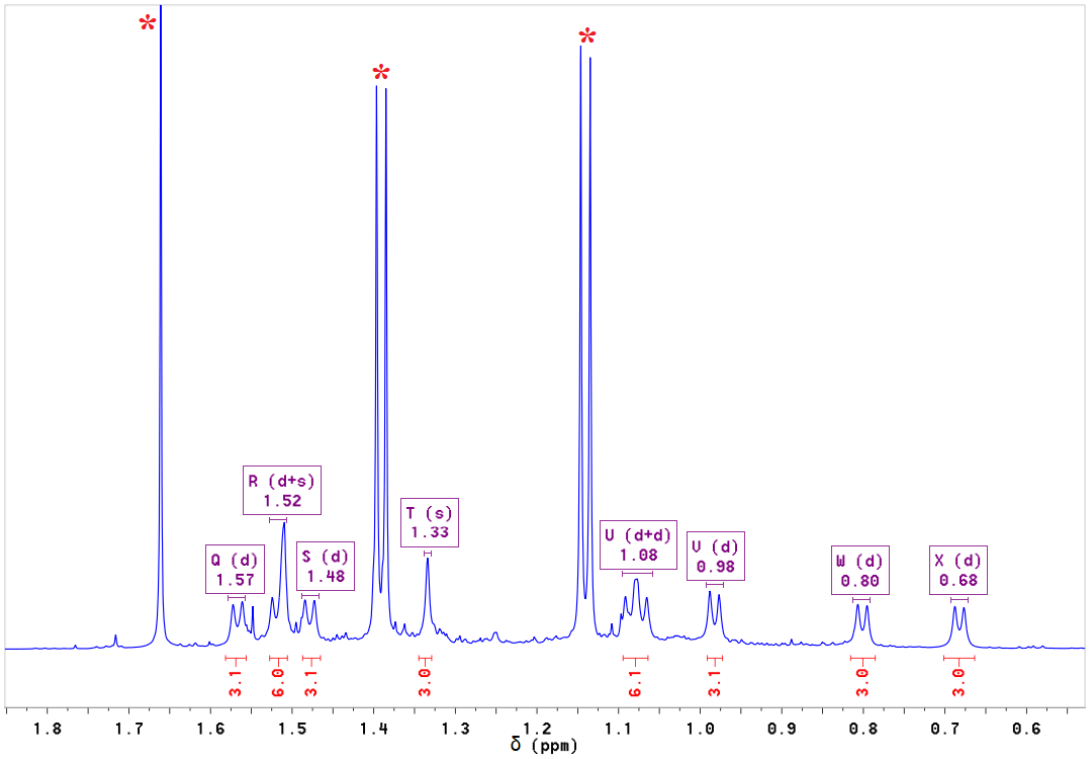

Figure S7. Selected strong field region of the ^{1}H NMR spectrum of the equilibrium with phenanthrene in C_6D_6.

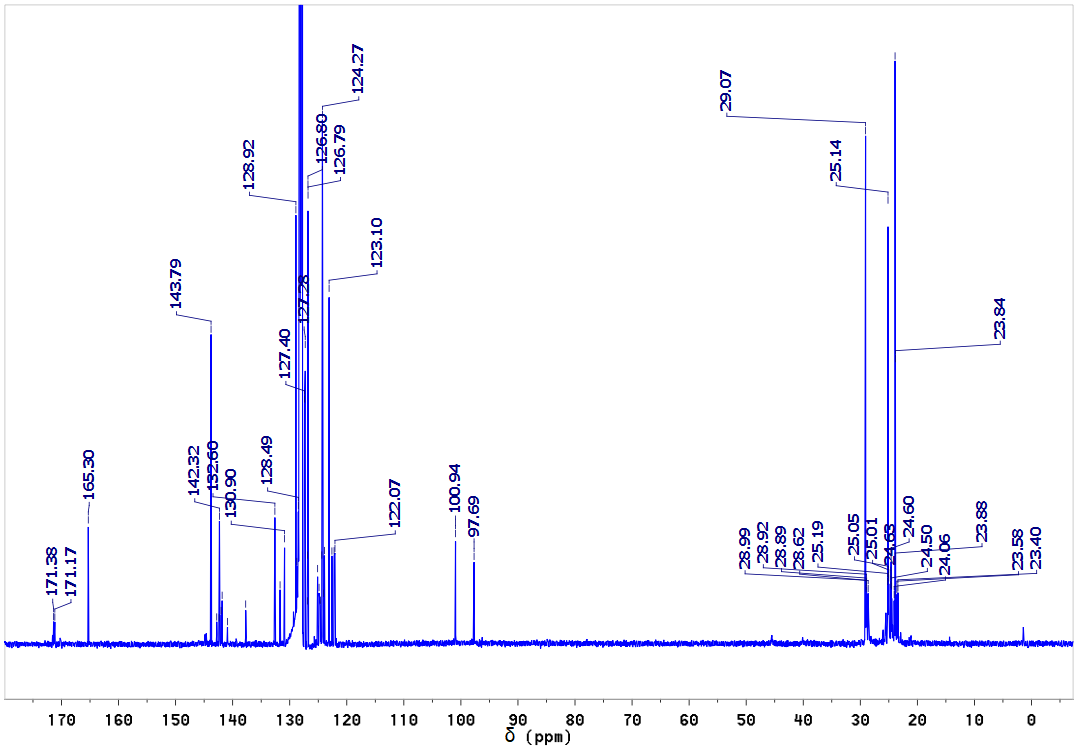

Figure S8. ^{13}C NMR spectrum of the equilibrium with phenanthrene in C_6D_6.

5. Dynamic equilibrium between 5 and triphenylene adduct 10

^{1}H NMR (600 MHz, C_6D_6) δ 8.56 (d, $^{3}J_{H\text{-}H}$ = 8.0 Hz, 2H, C_6H_4), 8.24 (dd, $^{3}J_{H\text{-}H}$ = 8.2, $^{4}J_{H\text{-}H}$ = 1.0 Hz, 2H, C_6H_4), 7.45 – 7.42 (m, 2H, C_6H_4), 7.39 – 7.37 (m, 2H, C_6H_4), 7.15 – 7.11 (m, 3H, C_6H_3), 6.41 – 6.33 (m, C_6H_3 3H), 5.88 (dd, $^{3}J_{H\text{-}H}$ = 4.7, $^{4}J_{H\text{-}H}$ = 3.3 Hz, 2H, C_6H_4), 4.83 (s, 1H), 4.50 (dd, $^{3}J_{H\text{-}H}$ = 4.3, $^{4}J_{H\text{-}H}$ = 3.7 Hz, 2H, C_6H_4), 3.30 (hept, $^{3}J_{H\text{-}H}$ = 6.7 Hz, 2H, $CH(CH_3)_2$), 2.81 (hept, $^{3}J_{H\text{-}H}$ = 6.7 Hz, 2H, $CH(CH_3)_2$), 1.55 (s, 3H, CCH_3), 1.53 ($^{3}J_{H\text{-}H}$ = 6.7 Hz, 6H, $CH(CH_3)_2$), 1.34 (s, 3H, CCH_3), 1.10 (d, $^{3}J_{H\text{-}H}$ = 6.7 Hz, 6H, $CH(CH_3)_2$), 0.93 (d, $^{3}J_{H\text{-}H}$ = 6.7 Hz, 6H, $CH(CH_3)_2$), 0.84 (d, $^{3}J_{H\text{-}H}$ = 6.7 Hz, 6H, $CH(CH_3)_2$).

^{13}C NMR (151 MHz, C_6D_6) δ 171.3 (CCH_3, q.), 165.3 (NacNacAl), 143.8 (NacNacAl), 142.5 (C_6H_3, q.), 142.3 (NacNacAl), 141.5 (C_6H_3, q.), 140.5 (C_6H_3, q.), 136.0 (C_6H_4, q.), 130.3 (triphenylene), 129.6 (C_6H_4, q.), 128.9 (C_6H_4, q.), 127.4 (triphenylene), 126.8 (C_6H_4), 126.0 (C_6H_3), 125.4 (C_6H_4), 124.8 (C_6H_3), 124.5 (C_6H_4), 124.3 (NacNacAl), 124.1 (C_6H_3), 123.7 (triphenylene), 123.14 (C_6H_4), 123.10 (C_6H_4), 100.9 (NacNacAl), 97.7 (CH), 40.9 (C_6H_4), 29.1 (NacNacAl), 28.9 ($CH(CH_3)_2$), 25.14 (NacNacAl), 25.10 ($CH(CH_3)_2$), 24.8 ($CH(CH_3)_2$), 24.7 (CCH_3), 24.3 (CCH_3), 23.9 (NacNacAl), 23.8 (NacNacAl), 23.7 ($CH(CH_3)_2$), 23.6 ($CH(CH_3)_2$).

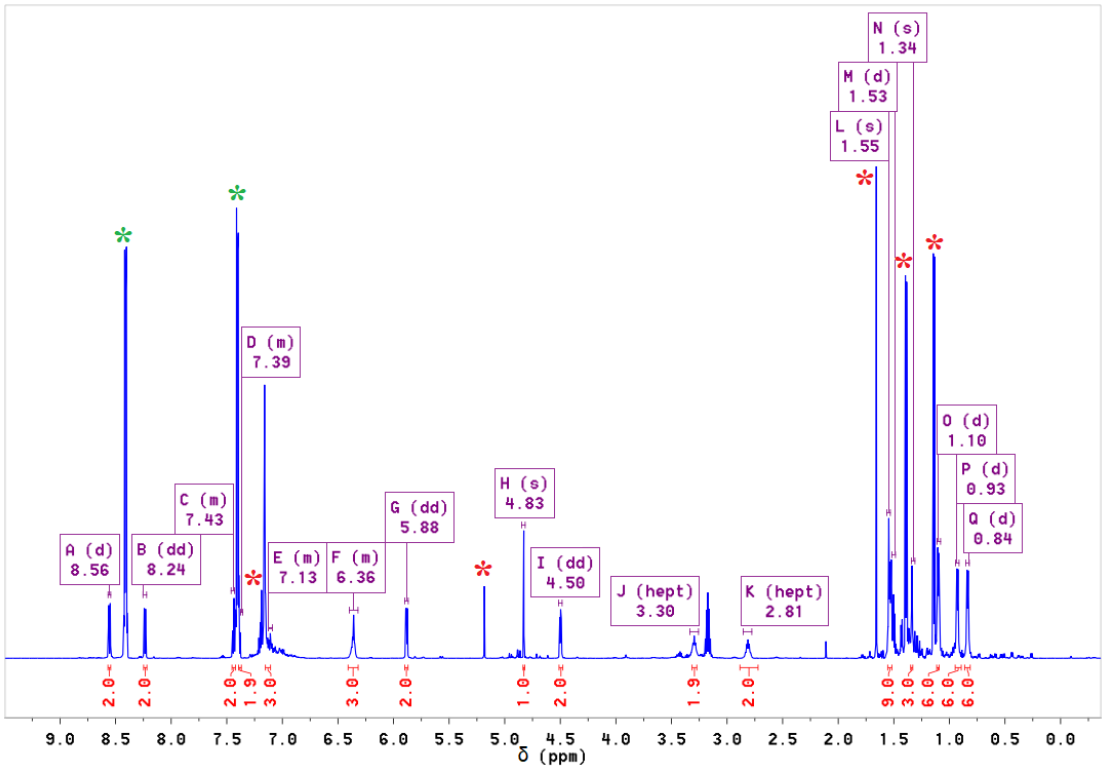

Figure S9. ^{1}H NMR spectrum of the equilibrium with triphenylene in C_6D_6.

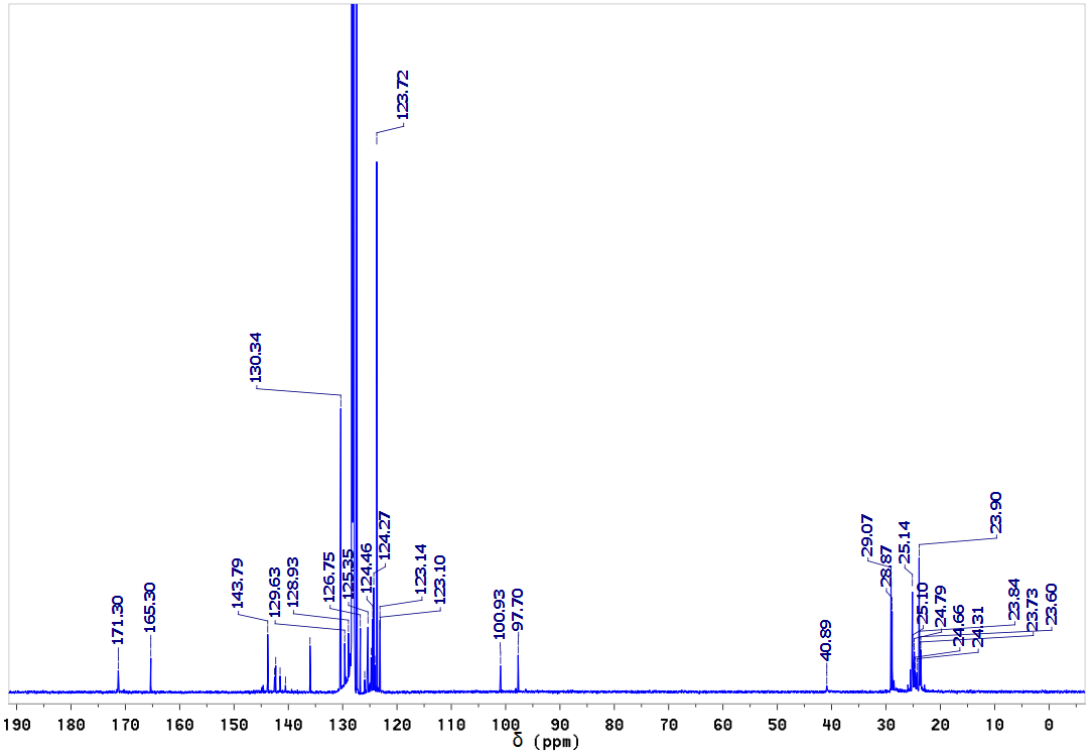

Figure S10. ^{13}C NMR spectrum of the equilibrium with triphenylene in C_6D_6.

6. Dynamic equilibrium between 5 and fluoranthene adduct 11

^{1}H NMR (600 MHz, C_6D_6) δ: 8.11 (d, $^{3}J_{H\text{-}H}$ = 7.5 Hz, 1H, $C_{10}H_6$ (arom.)), 7.96 (d, $^{3}J_{H\text{-}H}$ = 7.5 Hz, 1H, C_6H_4), 7.53 (td, $^{3}J_{H\text{-}H}$ = 7.5, $^{4}J_{H\text{-}H}$ = 1.0 Hz, 1H, $C_{10}H_6$ (arom.)), 7.41 (m, 1H+1H, C_6H_4+$C_{10}H_6$ (arom.)), 7.15 – 7.11 (m, 3H, C_6H_3), 6.98 (m, 2H, C_6H_3), 6.92 (t, $^{3}J_{H\text{-}H}$ = 7.3 Hz, 1H, C_6H_4), 6.76 (dd, $^{3}J_{H\text{-}H}$ = 6.6, $^{4}J_{H\text{-}H}$ = 2.3 Hz, 1H, C_6H_3), 6.68 (d, $^{3}J_{H\text{-}H}$ = 7.1 Hz, 1H, C_6H_4), 6.01 (dd, $^{3}J_{H\text{-}H}$ = 6.8, $^{4}J_{H\text{-}H}$ = 1.5 Hz, 1H, $C_{10}H_6$), 5.54 (t, $^{3}J_{H\text{-}H}$ = 6.8 Hz, 1H, $C_{10}H_6$), 4.74 (s, 1H, C*H*), 3.76 (dd, $^{3}J_{H\text{-}H}$ = 6.8, $^{4}J_{H\text{-}H}$ = 1.5 Hz, 1H, $C_{10}H_6$), 3.69 (hept, $^{3}J_{H\text{-}H}$ = 6.8 Hz, 1H, C*H*$(CH_3)_2$), 3.37 (hept, $^{3}J_{H\text{-}H}$ = 6.8 Hz, 1H, C*H*$(CH_3)_2$), 3.25 (hept, $^{3}J_{H\text{-}H}$ = 6.8 Hz, 1H, C*H*$(CH_3)_2$), 1.60 (d+d, $^{3}J_{H\text{-}H}$ = 6.8 Hz, 3H+3H, CH(C*H*$_3)_2$), 1.56 (hept, $^{3}J_{H\text{-}H}$ = 6.8 Hz, 1H, C*H*$(CH_3)_2$) 1.46 (s+d, $^{3}J_{H\text{-}H}$ = 6.8 Hz, 3H+3H, CC*H*$_3$+CH(C*H*$_3)_2$), 1.17 (d, $^{3}J_{H\text{-}H}$ = 6.8 Hz, 3H, CH(C*H*$_3)_2$), 1.14 (s, 3H, CC*H*$_3$), 1.08 (d, $^{3}J_{H\text{-}H}$ = 6.8 Hz, 3H, CH(C*H*$_3)_2$), 1.01 (d, $^{3}J_{H\text{-}H}$ = 6.8 Hz, 3H, CH(C*H*$_3)_2$), 0.87 (d, $^{3}J_{H\text{-}H}$ = 6.8 Hz, 3H, CH(C*H*$_3)_2$), 0.52 (d, $^{3}J_{H\text{-}H}$ = 6.8 Hz, 3H, CH(C*H*$_3)_2$).

^{13}C NMR (151 MHz, C_6D_6) δ 172.4 (*C*CH_3, q.), 172.0 (*C*CH_3, q.), 165.3 (NacNacAl), 149.1 (*C*$_6H_4$, q.), 148.8 (*C*$_6H_4$, q.), 144.5 (*C*$_6H_3$, q.), 143.8 (NacNacAl), 143.61 (*C*$_6H_3$, q.), 143.58 (*C*$_{10}H_6$, q.), 142.5 (*C*$_6H_3$, q.), 142.3 (NacNacAl), 142.1 (*C*$_6H_3$, q.), 142.0 (*C*$_6H_3$, q.), 140.9 (*C*$_6H_3$, q.), 140.0 (Fluoranthene), 138.2 ($C_{10}H_6$, q.), 137.5 (Fluoranthene), 133.0 (Fluoranthene), 130.6 (Fluoranthene), 129.7 (*C*$_{10}H_6$, q.), 127.4 (NacNacAl), 127.2 (*C*$_6H_3$), 126.9 (Fluoranthene), 125.2 ($C_{10}H_6$, arom.), 124.9 (C_6H_3), 124.8 (*C*$_6H_3$), 124.7 (*C*$_6H_4$), 124.42 (*C*$_{10}H_6$), 124.35 (*C*$_6H_3$), 124.3 (NacNacAl), 124.0 (C_6H_3), 123.7 (*C*$_{10}H_6$, arom.), 123.6 (*C*$_{10}H_6$, arom.), 122.3 (*C*$_{10}H_6$), 122.0 (*C*$_6H_4$), 121.9 (Fluoranthene), 120.4 (Fluoranthene), 117.8 (*C*$_6H_4$), 114.3 (*C*$_6H_4$), 100.9 (NacNacAl), 98.7 (*C*H), 43.4 (*C*$_{10}H_6$) (visible in HSQC only) 29.1 (*C*H$(CH_3)_2$), 29.1 (NacNacAl), 29.0 (*C*H$(CH_3)_2$), 28.9 (*C*H$(CH_3)_2$), 28.2 (*C*H$(CH_3)_2$), 25.41 (CH(*C*H$_3)_2$), 25.36 (CH(*C*H$_3)_2$), 25.14 (NacNacAl), 25.11 (CH(*C*H$_3)_2$), 25.08 (CH(*C*H$_3)_2$), 25.0 (CH(*C*H$_3)_2$), 24.9 (CH(*C*H$_3)_2$), 24.44 (CH(*C*H$_3)_2$), 24.37 (C*C*H$_3$), 24.2 (CH(*C*H$_3)_2$), 24.1 (C*C*H$_3$), 23.9 (NacNacAl), 23.8 (NacNacAl).

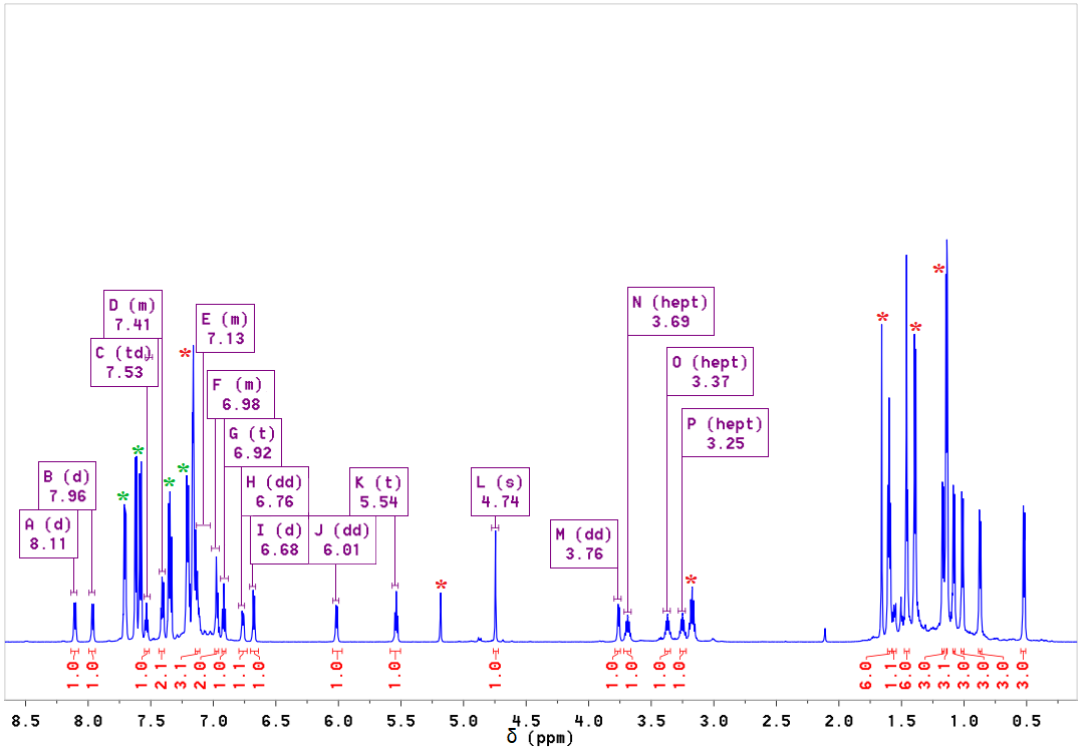

Figure S11. ^{1}H NMR spectrum of the equilibrium with fluoranthene in C_6D_6.

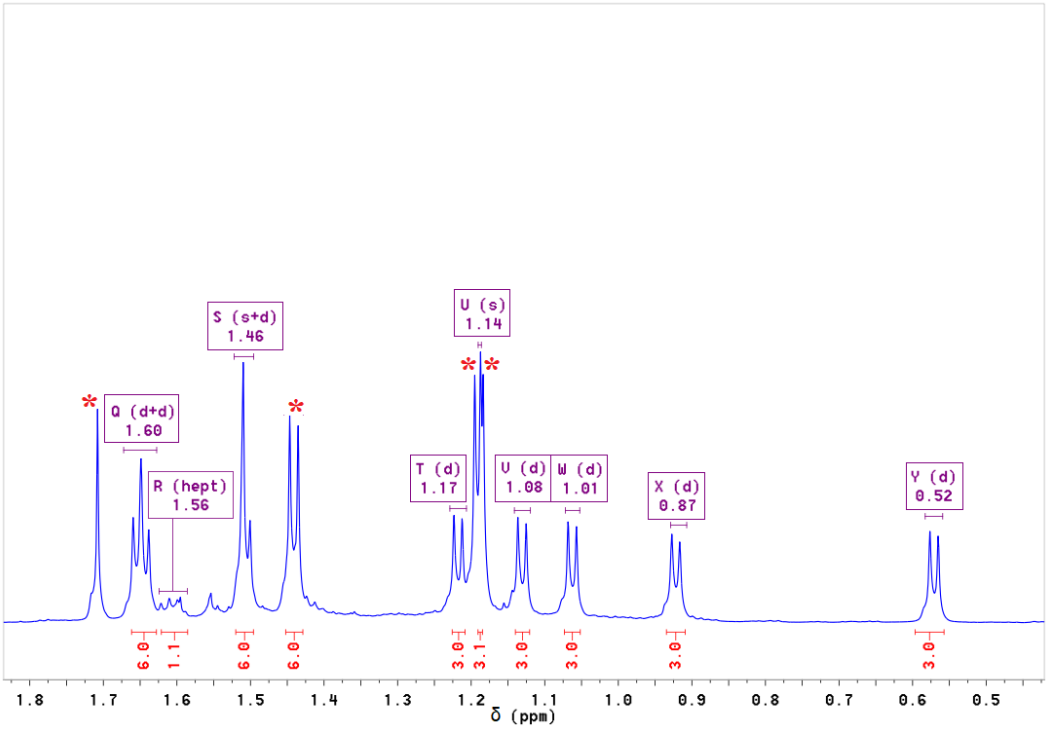

Figure S12. Selected strong field region of the ^{1}H NMR spectrum of the equilibrium with fluoranthene in C_6D_6.

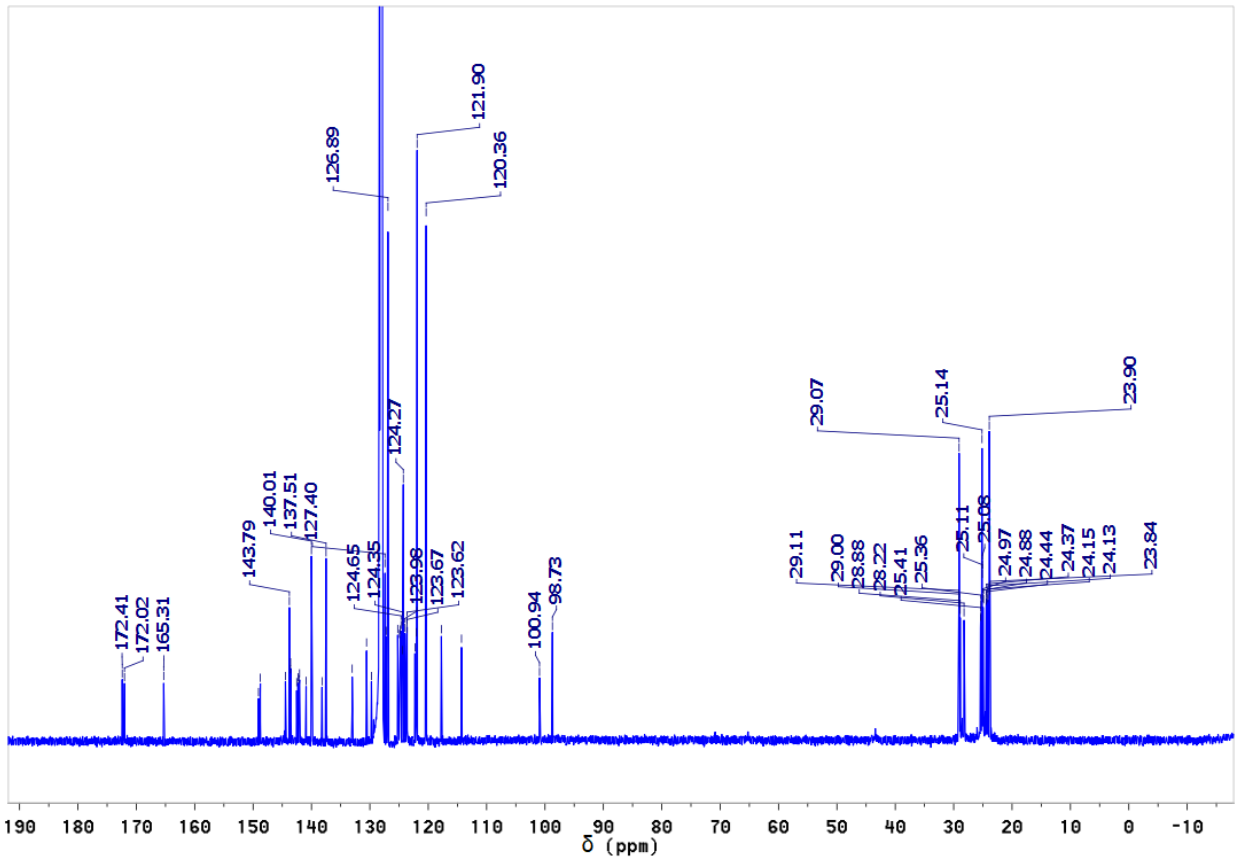

Figure S13. ^{13}C NMR spectrum of the equilibrium with fluoranthene in C_6D_6.

7. EXSY kinetic studies on anthracene complex 8a

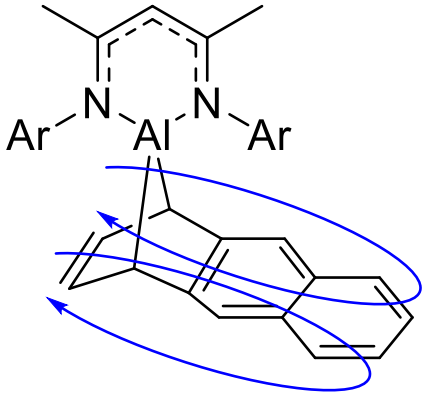

Figure S14. Illustration depicting rotational isomerism of species **8a**.

Isolated species **8a** was dissolved in toluene-d_8 and poured in the NMR tube filled with dry N_2, which was then inserted in the Bruker Avance AV 600 Digital NMR spectrometer with a 14.1 Tesla Ultrashield Plus magnet. The sample was held at each temperature for 10 minutes prior to data acquisition. Two doublets at 698.965 Hz and 594.717 Hz assigned to CH(CH_3) moiety were selected for estimation of rate constants, as exchanging in EXSY. The variation of d8-delay times changes intensity ratio between exchanging signals allowing one to determine rate constants of the rotational exchange. Five points were obtained for five different temperatures. Eyring plot (**Figure S20**) was fitted to a linear function with 99.9992% reliability.

Table S1. Experimental data of EXSY kinetic experiment.

T, K	*1/T, K^{-1}*	*Delays, s*	*Signal [A] 698.965 Hz*	*Signal [B] 594.717 Hz*	*[A]/[B]*	*k, s^{-1}*
289.7	0.003452	0	0	0	0	2.081
		0.05	9.5227	90.4773	0.1052496	
		0.04	7.7790	92.2210	0.0843517	
		0.03	5.9276	94.0724	0.063011	
		0.02	4.2415	95.7585	0.0442937	
		0.01	2.2700	97.7300	0.0232273	
285.3	0.003505	0	0.0000	0.0000	0	1.1673
		0.1	10.4654	89.5346	0.1168867	
		0.08	8.6493	91.3507	0.0946824	
		0.06	6.6813	93.3187	0.0715966	
		0.04	4.5117	95.4883	0.0472487	
		0.02	2.4627	97.5373	0.0252488	
295.0	0.00339	0	0.0000	0.0000	0	3.8639
		0.01	4.0116	95.9884	0.0417925	
		0.005	2.3758	97.6242	0.0243362	
		0.003	1.6282	98.3718	0.0165515	
		0.015	5.8379	94.1621	0.0619984	
		0.02	7.3053	92.6947	0.0788103	
		0.025	9.0819	90.9181	0.099891	
300.1	0.003332	0	0.0000	0.0000	0	6.5167
		0.003	2.7184	97.2816	0.0279436	
		0.006	4.1940	95.8060	0.043776	
		0.009	5.7345	94.2655	0.0608335	
		0.012	7.5296	92.4704	0.0814271	
		0.015	9.2023	90.7977	0.1013495	
304.9	0.00328	0	0.0000	0	0	11.272
		0.003	3.6501	96.3499	0.0378838	
		0.005	5.9052	94.0948	0.062758	
		0.007	7.6316	92.3684	0.0826213	
		0.009	9.4206	90.5794	0.1040038	
		0.011	11.0992	88.9008	0.1248493	

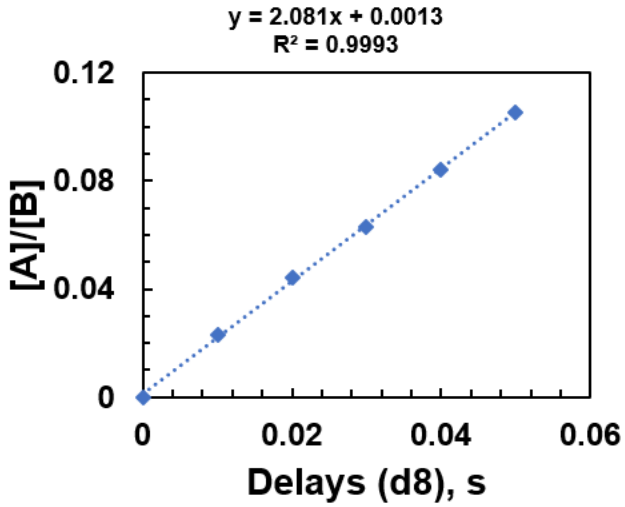

Figure S15. [A]/[B] vs. Delays plot at 289.7 K.

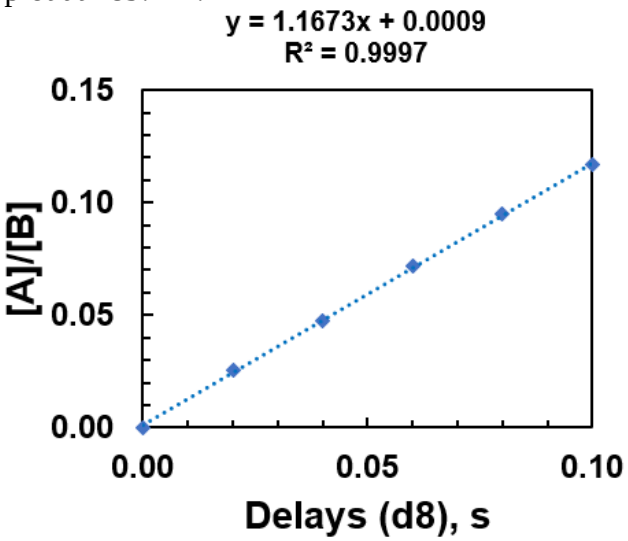

Figure S16. [A]/[B] vs. Delays plot at 285.3 K.

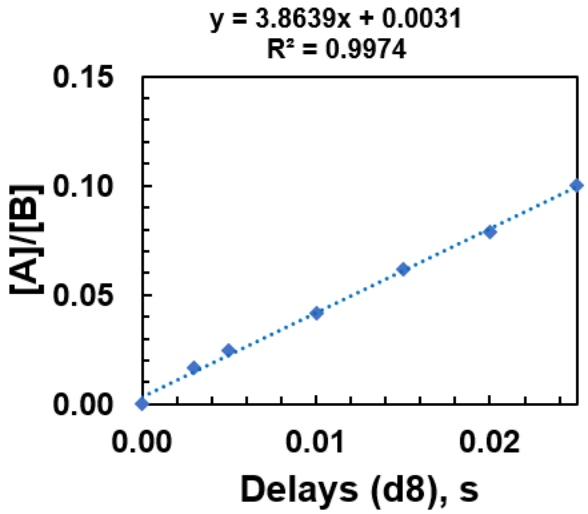

Figure S17. [A]/[B] vs. Delays plot at 295.0 K.

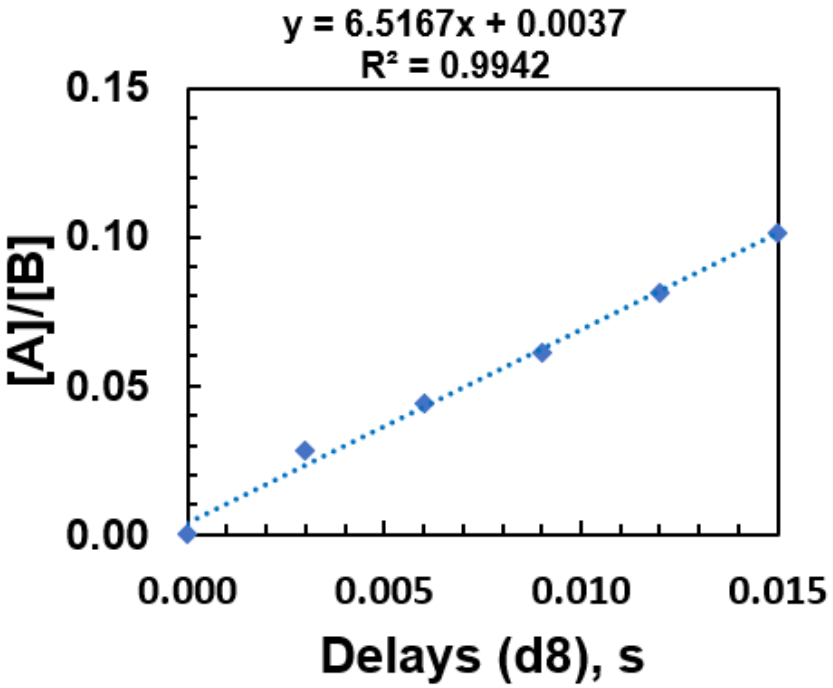

Figure S18. [A]/[B] vs. Delays plot at 300.1 K.

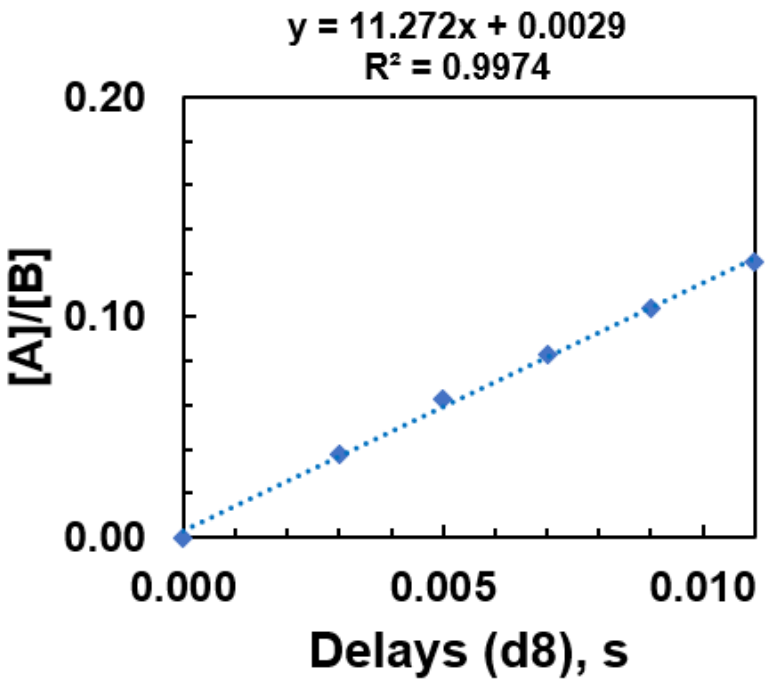

Figure S19. [A]/[B] vs. Delays plot at 304.9 K.

Table S2. Processed dataset for determination of Δ_rH, Δ_rS, E_a of the rotational exchange.

T, K	*1/T, K^{-1}*	*k, s^{-1}*	*ln[k/T]*	*ln[K]*	*Slope*	*Intercept*	*k(Boltz)*
289.7	0.0034518	2.081	-4.935997357	0.732848547	-9656.6	28.373	1.38065E-23
285.3	0.0035051	1.1673	-5.498847869	0.15469339	Δ_rH, J/mol	Δ_rS, J/mol K	E_a, J
295	0.0033898	3.8639	-4.33529832	1.351677036	80284.9724	38.352482	82735.9396
300.1	0.0033322	6.5167	-3.82974764	1.874368113	80.3 (kJ/mol)	38 J/molK	82.7 kJ
304.9	0.0032798	11.272	-3.297662079	2.422321775			

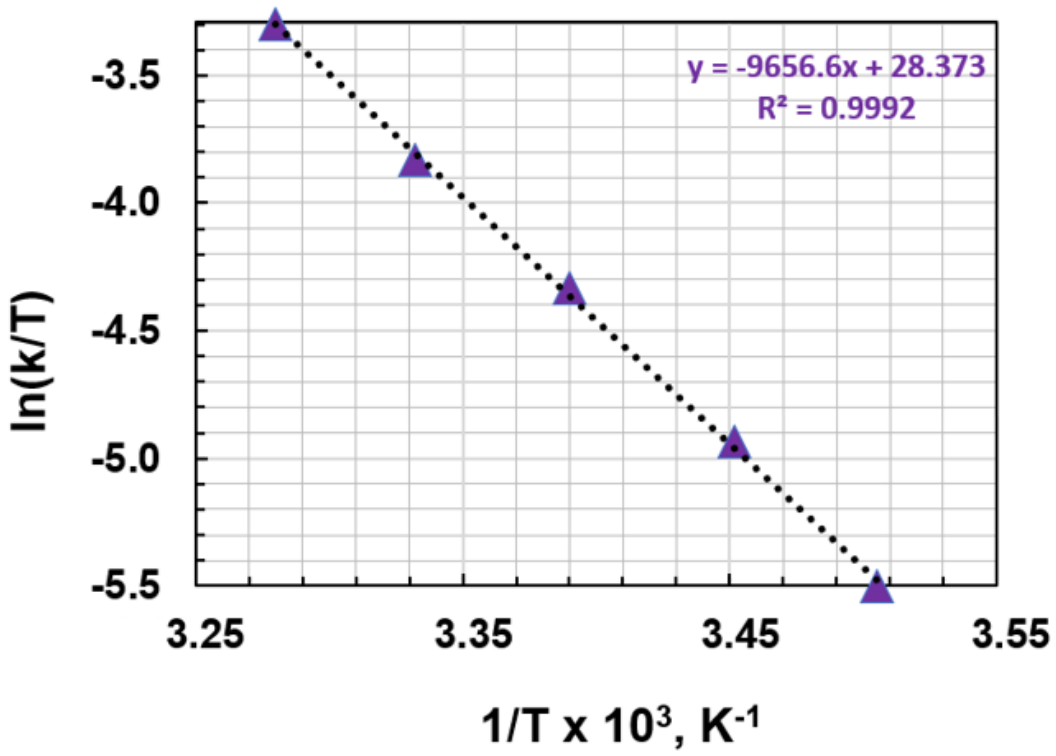

Figure S20. Eyring plot.

8. Equilibrium studies on fluoranthene adduct 11

Equilibrium mixture with fluoranthene was prepared by mixing NacNacAl **5** with fluoranthene. Hexamethyldisilane (1.9 µl, 9.3 µmol) was used as a reference. Prepared solution in toluene-d_8 was injected into the sealed NMR tube that was inserted into the NMR machine. The sample was statically heated at each temperature for 24 hours prior to data acquisition. The data was collected at eight different temperatures from 300.65 to 318.15 K.

Table S3. Experimental VT-NMR data obtained for estimation of equilibrium constant K**.**

Temperature regime		*Masses, g. (referenced to HMDS)*			*Equillibrium const.*	
T, K	***1/T, K^{-1}***	***Fluoranthene***	***Al(I)***	***Al(III)***	***$K_{eq.}$***	***ln($K_{eq.}$)***
300.65	3.33E-03	1.53E-03	1.74E-03	3.12E-03	1174	7.1
303.15	3.30E-03	1.56E-03	1.88E-03	2.94E-03	1002	6.9
305.65	3.27E-03	1.61E-03	2.02E-03	2.77E-03	854	6.8
308.15	3.25E-03	1.66E-03	2.17E-03	2.61E-03	721	6.6
310.65	3.22E-03	1.69E-03	2.29E-03	2.42E-03	623	6.4
313.15	3.19E-03	1.75E-03	2.47E-03	2.25E-03	520	6.3
315.65	3.17E-03	1.79E-03	2.63E-03	2.07E-03	440	6.1
318.15	3.14E-03	1.86E-03	2.82E-03	1.93E-03	370	5.9

Enthalpy $\Delta_r H°$ and $\Delta_r S°$ values were derived from processing of the data in keeping with the following equations:

$$-RT \ln K_{eq} = \Delta_r H^\circ - T\Delta_r S^\circ \quad \text{eq. (1)}$$

$$\ln K_{eq} = -\frac{\Delta_r H^\circ}{R} \cdot \frac{1}{T} + \frac{\Delta_r S^\circ}{R} \quad \text{eq. (2)}$$

$\Delta_r H°$ = -52 kJ/mol, $\Delta_r S°$ = -115 J/mol K

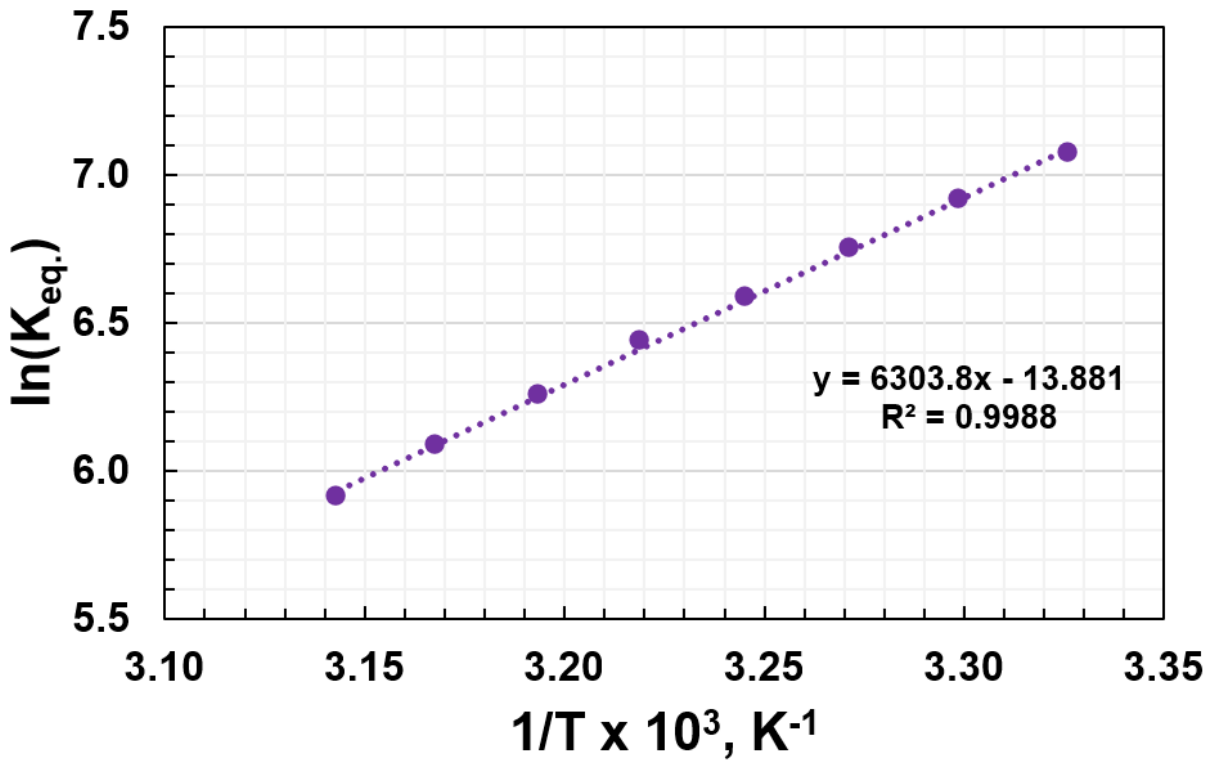

Figure S21. Van't Hoff plot for the system **5** – fluoranthene.

9. Crystallographic details

Suitable single crystals were mounted on a glass microloop covered with perfluoroether oil (Paratone® N). Crystallographic data were collected on Bruker APEX-II CCD diffractometer equipped with an Oxford Cryosystems low-temperature device operating at 150.0(1) K. Generic φ and ω scans (MoKα, λ = 0.71073 Å) were used for the data measurement. The diffraction patterns were indexed, and the unit cells refined with SAINT (Bruker, V.8.34A, after 2013) software. Data reduction, scaling and absorption correction were performed with SAINT and SADABS software (Bruker, 8.34A after 2013). A multi-scan absorption correction was applied within SADABS-2014/4 (Bruker, 2014/4). Space group determination was based upon analysis of systematic absences, *E* statistics, and successful refinement of all structures. The structures were solved by ShelXT (Sheldrick, 2015) structure solution program with *Intrinsic phasing* algorithm and refined with *Least squares* method by minimization of $\Sigma w(F_0^2-F_c^2)^2$. SHELXL weighting scheme was used under 2018/3 version of ShelXL (Sheldrick, 2015). Structure solution, refinement and CIF compilation was performed within Olex^{2}SyS software (Dolomanov, 2009). All non-hydrogen atoms were refined anisotropically. The positions of the hydrogen atoms were calculated geometrically and refined using the riding model. Neutral atom scattering factors for all atoms were taken from the International Tables for Crystallography. All of the crystallographic data were deposited in the Cambridge structural database.

Table S4. Crystal data and structure refinement for compound **7**.

Identification code	Anton_naph_150K
Empirical formula	$C_{39}H_{49}AlN_2$
Formula weight	572.78
Temperature (K)	150.0(1)
Crystal system	Monoclinic
Space group	$P2_1/c$
a (Å)	15.4217(15)
b (Å)	13.4391(13)
c (Å)	18.0681(18)
α (°)	90
β (°)	91.384(3)
γ (°)	90
Volume ($Å^3$)	3743.6(6)
Z	4
ρ_{calc} (g cm^{-3})	1.016
μ (mm^{-1})	0.080
F(000)	1240.0
Crystal size	0.135×0.115×0.105
Crystal shape	irregular
Crystal color	Yellow
Radiation	MoKα (λ = 0.71073 Å)
2θ range for data collection (°)	2.642 to 54.206
Index ranges	$-14 \leq h \leq 19$ $-17 \leq k \leq 17$ $-23 \leq l \leq 23$
Reflections collected	48380
Independent reflections	8244 R_{int} = 0.0725, R_{sigma} = 0.0550
Data/Restraints/Parameters	8244/6/401
Goodness-of-fit on F^2	1.064
Final R indexes [I≥2σ (I)]	R_1 = 0.0824, wR_2 = 0.1691
Final R indexes [all data]	R_1 = 0.1079, wR_2 = 0.1829
Largest diff. peak/hole (*e* $Å^{-3}$)	0.48/-0.41
Flack parameter	N/A

Table S5. Crystal data and structure refinement for compound **8c**.

Identification code	Anton_Anthr_Cs_150K_0m
Empirical formula	$C_{43}H_{53}AlN_2O$
Formula weight	640.85
Temperature (K)	150.0(1)
Crystal system	Monoclinic
Space group	$P2_1/n$
a (Å)	10.6800(12)
b (Å)	15.4361(16)
c (Å)	22.0580(20)
α (°)	90
β (°)	93.826(3)
γ (°)	90
Volume ($Å^3$)	3628.3(7)
Z	4
ρ_{calc} (g cm^{-3})	1.173
μ (mm^{-1})	0.091
F(000)	1384.0
Crystal size	0.176×0.155×0.153
Crystal shape	Plate
Crystal color	Yellow
Radiation	MoKα (λ = 0.71073 Å)
2θ range for data collection (°)	4.134 to 51.362
Index ranges	$-13 \leq h \leq 12$ $-18 \leq k \leq 18$ $-26 \leq l \leq 22$
Reflections collected	36244
Independent reflections	6841 $R_{int} = 0.0368$, $R_{sigma} = 0.0297$
Data/Restraints/Parameters	6841/568/433
Goodness-of-fit on F^2	1.120
Final R indexes [I≥2σ (I)]	$R_1 = 0.0885$, $wR_2 = 0.1876$
Final R indexes [all data]	$R_1 = 0.1020$, $wR_2 = 0.1953$
Largest diff. peak/hole (*e* $Å^{-3}$)	0.91/-0.54
Flack parameter	N/A